eNeuro

Research Article: New Research | Disorders of the Nervous System

Sex-specific differences in motor unit remodeling in a mouse model of ALS

https://doi.org/10.1523/ENEURO.0388-19.2020

Cite as: eNeuro 2020; 10.1523/ENEURO.0388-19.2020

Received: 24 September 2019
Revised: 20 January 2020
Accepted: 27 January 2020

1. **Title: Sex-specific differences in motor unit remodeling in a mouse model of ALS**

2. **Abbreviated Title: Sex affects motor unit remodeling in an ALS model**

3. **Authors:** Éric Martineau[1,2*], Adriana Di Polo[1,3], Christine Vande Velde[1,3], Richard Robitaille[1,4]

Affiliations:
[1] Département de neurosciences, Université de Montréal, PO box 6128, Station centre-ville, Montréal, Québec, Canada, H3C 3J7
[2] Centre de recherche du CHU Sainte Justine, 3175, chemin de la Côte-Ste-Catherine, Montréal Québec, Canada, H3T 1C5
[3] Centre de recherche du Centre Hospitalier de l'Université de Montréal (CRCHUM), 900 Rue Saint-Denis, Montréal, Québec, Canada, H2X 0A9.
[4] Groupe de recherche sur le système nerveux central, Université de Montréal.

4. **Author Contributions**: EM and RR designed research; EM performed research; EM analyzed data; ADP and CVV contributed unpublished reagents/tools; EM, ADP, CVV and RR wrote the paper;

5. *To whom correspondence should be addressed: eric.martineau.3@umontreal.ca

6. Number of Figures: 3
7. Number of Tables: 2
8. Number of Multimedia: 0
9. Number of words for Abstract:175
10. Number of words for Significance Statement: 111
11. Number of words for Introduction: 476
12. Number of words for Discussion: 1049

13. **Acknowledgements**: We thank Sarah Peyrard and Joanne Vallée for their crucial help with animal husbandry, logistics and technical support.

14. **Conflict of Interest**: Authors report no conflict of interest

15. **Funding sources**: This work was funded by grants from the Canadian Institutes for Health Research (R.R. MOP-111070; A.D.P. PJT-376483), Robert Packard Center for ALS Research (R.R.), Canadian Foundation of Innovation (R.R., C.V.V), ALS Society of Canada (C.V.V.), Muscular Dystrophy Association (C.V.V.) and an infrastructure grant from the Fonds Recherche Québec-Santé Leader Opportunity Fund to the GRSNC. C.V.V. is an FRQS Senior Research Scholar. A.D.P. is a Canada Research Chair in Glaucoma and Age-Related Neurodegeneration. É.M. held a doctoral studentship from the ALS Society of Canada.

Abstract

Progressive loss of neuromuscular junctions (NMJ) is an early event in amyotrophic lateral sclerosis (ALS), preceding the global degeneration of motor axons and being accompanied by new axonal sprouting within the same axonal arbor. Some aspects of ALS onset and progression seem to be affected by sex in animal models of the disease. However, whether there are sex-specific differences in the pattern or time course of NMJ loss and repair within single motor axons remains unknown. We performed further analysis of a previously published *in vivo* dataset, obtained from male and female SOD1^{G37R} mice. We found that NMJ losses are as frequent in male and female motor axons but, intriguingly, axonal sprouting is more frequent in female than male mice, resulting in a net increase of axonal arborization. Interestingly, these numerous new axonal branches in female mice are associated with a slightly faster decline in grip strength, increased NMJ denervation, and reduced α-motor neuron survival. Collectively, these results suggest that excessive axonal sprouting and motor-unit expansion in female SOD1^{G37R} mice are maladaptive during ALS progression.

Significance Statement

Sex-specific differences in ALS progression have been identified in patients and in some animal models of the disease. However, the physio-pathological changes underlying these disparities remain poorly defined. In this study, we identified that the pattern of motor axon retraction and regrowth in skeletal muscles is a novel factor to consider in our understanding of sex-linked differences in ALS. Analysis of single motor axons in a model of ALS identified that female motor axons were more likely to form compensatory branches, which was associated with a worse phenotype. These surprising findings highlight the necessity to more systematically evaluate the prevalence of sex-specific differences across animal models of ALS and in patients.

68 **Introduction**

69 ALS is a neurodegenerative disease affecting motor neurons. The early dysfunction and
70 loss of NMJs is a key event in patients and animal models of the disease (Fischer et al., 2004;
71 Pun et al., 2006; Armstrong and Drapeau, 2013a, b; Clark et al., 2016; Tallon et al., 2016;
72 Tremblay et al., 2017; Chand et al., 2018). A recent study has shown in SOD1^{G37R} mice that
73 NMJ loss within single motor-units (MUs), defined as a motor neuron and the muscle fibers it
74 innervates, is initially slow and asynchronous (Martineau et al., 2018). These losses are
75 accompanied by the formation of new collateral axonal branches (expansions), reinnervating
76 other nearby NMJs (Martineau et al., 2018). Importantly, this period of dynamism precedes
77 global axonal degeneration by several weeks, revealing that NMJ loss is initially a local process
78 involving constant axonal retraction and growth.

79 Sex-specific differences in disease onset and progression have been observed in patients
80 and in some animal models of ALS (McCombe and Henderson, 2010). In humans, ALS onset
81 tends to be delayed in women with most studies reporting a delay between 0.9 and 5.5 years in
82 the mean or median age at diagnosis (McCombe and Henderson, 2010; Chen et al., 2015). This
83 tendency is further reflected in the sex ratio for the incidence of ALS. Indeed, while the overall
84 male-to-female ratio is around 1.3, the ratio is 3.98:1 for onsets occurring before 49 years of age
85 and gradually equalizes with age (Manjaly et al., 2010; McCombe and Henderson, 2010).
86 Similarly, disease onset is slightly delayed in SOD1^{G93A} female mice compared to male mice
87 (Pfohl et al., 2015). However, whether sex affects neuromuscular dysfunction and NMJ loss in
88 ALS remains ill-defined. Previous studies using electromyographic recordings did not identify
89 sex-specific differences in the global time course and pattern of motor axon loss in SOD1^{G93A}
90 mice (Hegedus et al., 2009) or in ALS patients (McComas et al., 1971; Dengler et al., 1990;

Dantes and McComas, 1991; Schmied et al., 1999). Interestingly though, a recent study identified that women with ALS were twice as likely of having antibodies against two NMJ components, agrin and LRP4 (Rivner et al., 2017). Furthermore, Moloney and colleagues (2017) identified sex-specific differences in botulinum toxin-induced axonal sprouting in mice, with female mice notably exhibiting more sprouting from ALS-vulnerable fast-fatigable MUs. These recent findings raise the possibility that sex-specific differences may impact local NMJ dynamism in ALS, which could be an important factor to consider for therapeutic development.

To address this unexplored question, we examined if NMJ denervation and reinnervation within single motor axons occur similarly between male and female SOD1^{G37R} mice. We found that motor axons were more likely to form new axonal branches in female than in male SOD1^{G37R} mice. Interestingly, these compensatory expansions were associated with increased neuronal loss and NMJ denervation in female mice, suggesting that they may be detrimental to disease progression.

105 ## Material and Methods

106 **Animals**

107 SOD1^{G37R}/YFP (*SOD1*$^{+/-}$; YFP$^{+/-}$) transgenic mice were previously described (Martineau et al.,
108 2018). Briefly, they were obtained by breeding male lox*SOD1*^{G37R} mice (RRID:MGI:3629226)
109 with heterozygote female *Thy1*-YFP, line H, mice (B6.Cg-Tg(Thy1-YFP)HJrs/J; The Jackson
110 laboratories, Bar Harbor, ME, stock number 003782; RRID:MGI: 3497947). *Thy1*-YFP mice
111 from line H were used due to their sparse expression of the yellow-fluorescent protein (YFP) in
112 lower motor neurons (Feng et al., 2000) allowing visualization of single motor axons. Parent
113 lines were maintained on a C57BL6/J background. Importantly, transmission of both transgenes
114 follows a Mendelian autosomal pattern of inheritance, ruling out the possibility that either
115 transgene is integrated on a sex chromosome. Disease progression and motor function were
116 monitored via weekly weight and grip strength measurements (BioSeb, FL BIO-GS3). Animals
117 were sacrificed using a lethal dose of isoflurane. All experiments were performed in accordance
118 with the guidelines of the Canadian Council on Animal Care, the Comité de Déontologie sur
119 l'Expérimentation Animale of Université de Montréal (protocol #18-040) and the CRCHUM
120 Institutional Committee for the Protection of Animals (protocol #N16008CVV and
121 #N15047ADPs).

122 **Repeated *in vivo* imaging and image analysis**

123 Procedures for the repeated *in vivo* imaging of the *Tibialis anterior* muscle and image analysis
124 were described in the original publication of the *in vivo* imaging dataset (Martineau et al., 2018)
125 DOI:10.7554/eLife.41973). Briefly, mice were imaged every 2 weeks, for 5 to 6 sessions (10 –
126 12 weeks). Mice were anesthetized with 2 – 3% isoflurane and the *Tibialis anterior* muscle was

127 exposed by making a rostro-caudal incision on the exterior face of the hindlimb. Postsynaptic
128 nAChRs were labeled by applying a non-blocking concentration of Alexa 594-conjugated α-
129 bungarotoxin (BTX, 5µg/mL, in sterile lactated Ringer for 10 minutes; Molecular Probes, Fisher
130 Scientific, Canada) on the first session. BTX was reapplied only when the labeling was too dim,
131 on session 5 or 6. Images were obtained using a Neo-sCMOS camera (Andor, UK) mounted on
132 an upright Optiphot-2 microscope (Nikon) equipped with a 20X water immersion objective (0.4
133 NA, Nikon, Japan). Excitation light and fluorescence emission were filtered using a Brightline
134 Pinkel filter set optimized for CFP/YFP/HcRed (CFP/YFP/HcRed-3X-A-000; Semrock, NY).
135 The wound was then close using 5-0 and 6-0 vicryl sutures and tissue glue (GLUture; Abbot
136 Laboratories, WPI, FL). Mice were administered Buprenorphine (3 µg/10 g body weight; every 8
137 hours, 3 doses; Temgesic, CEVA Animal Health Ltd, UK) by subcutaneous injections. All SOD1
138 animals with YFP-positive surface motor axons which could be reliably followed for at least
139 three sessions and with at least three NMJs near the surface were included in this dataset. The
140 vast majority of imaged motor axons belong to fast-fatigable MUs as previously reported for this
141 dataset (Martineau et al., 2018).

142 **Whole-mount NMJ immunolabeling and motor neuron counts**

143 Procedures for the whole-mount muscle and spinal cord immunostaining were previously
144 described in detail (Martineau et al., 2018). Images were acquired on a Zeiss LSM 880 confocal
145 microscope with a 20X water immersion objective (N.A. 1.0). No image manipulations were
146 performed after acquisition, except for linear contrast adjustments for figure presentation. Motor
147 neurons in both ventral horns were counted from 15 to 20 sections per animal, separated by at
148 least 90 µm. The Allan Brain Atlas Mouse Spinal cord reference set was used to ensure that all
149 analyzed sections were in the lumbar spinal cord. All ChAT-positive cells in the ventral horn

150 were considered as motor neurons. NeuN-positive motor neurons were counted as α-motor
151 neurons while NeuN-negative motor neurons were counted as γ-motor neurons (Shneider et al.,
152 2009; Lalancette-Hebert et al., 2016).

153 **Statistical analysis**

154 Comparison of the frequency of expansions and asynchronous losses between male and
155 female SOD1^{G37R} mice was performed by using a *multivariate GLM with Poisson's or logistic*
156 *distribution*. The cumulative number of expansions or the cumulative number of asynchronous
157 losses over the total number of NMJs innervated by that MU at any time points for each animal
158 were used as the dependent variables. A logistic distribution was used for asynchronous losses as
159 they represent a number of events over a define number of trials (number of imaged NMJs
160 innervated by that MU). Poisson's distribution was used for the expansions as they represent
161 events which occur over a period of observation (as opposed to a define number of trials). For
162 this analysis, the sample size (number of MU arbors) and the number of biological replicates
163 (number of animals) are indicated in the text. *P-values* smaller than 0.05 (α=5%) were
164 considered statistically significant. Analyses were performed in the SPSS 24.0.0.0 (IBM)
165 software.

166 When the effect of two or three independent variables were compared (Figure 2 and 3),
167 *two-* or *three-way ANOVAs* were used, with (for motor behavior and weight) or without repeated
168 measures (*RM;* for motor neuron counts). For the post-test, Tukey's multiple comparisons was
169 used (referred to as "*ANOVA post-test"*). For NMJ innervation (Figure 3), the main effects of
170 each variable were compared using a *GLM* with a logistic distribution and Holm-Sidak's
171 correction was applied to all pairwise comparisons for the post-test (referred to as "*GLM post-*
172 *test"*) as previously described (Tremblay et al., 2017). Data are presented as mean ± SEM in the

histograms and in the text. “N” represents the number of biological replicates (animals) while “n’ represents the number of observations (number of NMJs unless otherwise stated). *P-values* smaller than 0.05 (α=5%) were considered statistically significant. These analyses were performed in the GraphPad Prism 7.0 software, with the exception of the analysis for the NMJ innervation and the three-way ANOVAs with repeated measures which were made in SPSS 24.0.0.0. For the purpose of clarity, only essential main effects and post-hoc comparisons are presented in the text. All other comparisons are reported in Table 1 and 2 (main effects) or are represented in the graphs (post hoc comparisons).

181 **Results**

182 To investigate sex-linked differences in NMJ loss in ALS, we first asked if NMJ
183 denervation and axonal sprouting occurred similarly in male and female SOD1^{G37R}. We
184 previously reported that single motor axons in SOD1^{G37R} mice asynchronously retracted from
185 some NMJs over time (a process referred to as asynchronous NMJ losses), while also forming
186 new branches to innervate nearby postsynaptic sites (expansions) (Martineau et al., 2018). Here,
187 we took advantage of this open-access dataset and performed a secondary analysis comparing
188 motor axon dynamics between male and female SOD1^{G37R} mice.

189 This dataset was obtained by repeatedly imaging single MUs and their NMJs in the
190 *Tibialis anterior* during disease progression every two weeks for 5 to 6 sessions (56 - 76 days).
191 Single motor axons were visualized by using SOD1^{G37R} mice expressing the YFP in a subset of
192 motor neurons (SOD1^{G37R}/YFP-H mice) and postsynaptic nicotinic acetylcholine receptors were
193 labeled with Alexa594-conjugated BTX. A total of 253 NMJs, belonging to 19 different MU
194 arbors, (males: 102 NMJs, 9 MU arbors, 7 animals; females: 151 NMJs, 10 MU arbors, 4
195 animals) were followed. NMJ losses or axonal sprouting innervating new NMJs (expansions)
196 were recorded over time.

197 **MU expansions are more frequent in females SOD1^{G37R} mice**

198 Interestingly, we observed that MU dynamics were vastly different between males and
199 females (Figure. 1A-B). While a similar number of axonal branches retracted from postsynaptic
200 sites (complete asynchronous NMJ losses) in male and female mice over all imaging sessions
201 (Figure 1C-D, males: 12/102 NMJs (12%) vs females: 26/151 NMJs (17%); *GLM;* p=0.592),
202 female MUs were strikingly more likely to form expansions (Figure 1C-D, males: 14/102 NMJs
203 (14%) vs females: 62/151 NMJs (41%); *GLM*; p=0.004). This difference was so pronounced that

204 only female MUs exhibited a net increase in size, while expansions barely masked the losses in
205 male MUs (Figure. 1C-D; average MU size on session 6, males: 99 ± 31% vs females: 204 ±
206 58%). Moreover, male MUs exhibited slightly more partial losses (partial retraction of the motor
207 axon) than female MUs (males: 18/102 NMJs (18%) vs females: 12/151 NMJs (8%); *GLM*;
208 p=0.029). Importantly, these differences are not due to differences in observation times or in the
209 initial size of axonal arbors between sexes, i.e. more observations due to having observed one
210 group for a longer period of time or having imaged larger arbors, as these parameters were
211 comparable between groups (females MUs: 58 sessions, 88 initial NMJs vs males MUs: 48
212 sessions, 88 initial NMJs).

213 **Grip strength, but not body weight, declines slightly faster in female SOD1^{G37R} mice**

214 To investigate whether these differences in MU dynamics were associated with
215 differences in disease progression in this mouse line, we analyzed the disease course of male and
216 female SOD1^{G37R} mice during the symptomatic phase by using two well-described and reliable
217 methods: all-limb grip strength and body weight (Figure 2 and Table 1) (Lobsiger et al., 2009;
218 Lobsiger et al., 2013; Mesci et al., 2015). Male and female SOD1^{G37R}/YFP mice exhibited a
219 parallel, age-dependent, decline in body weight relative to sex-matched WT/YFP animals
220 (Figure 2A and Table 1, *RM three-way ANOVA*; interaction between time and genotype:
221 p<0.001; interaction between time, genotype and sex: p=0.397), as previously reported (Lobsiger
222 et al., 2013). Surprisingly though, decline in all-limb grip strength was observable approximately
223 a month earlier in female than in male SOD1^{G37R}/YFP mice (Figure 2B and Table 1; *RM three-*
224 *way ANOVA*; interaction between time, genotype and sex: p=0.011). Hence, motor deficits occur
225 earlier in female SOD1^{G37R}/YFP mice compared to male mice.

226 **Motor neuron loss and NMJ denervation are exacerbated in female SOD1^{G37R} mice**

227 To further validate this tendency, NMJ innervation in the *Tibialis anterior* and α- and γ-
228 motor neuron survival in the lumbar spinal cord of male and female SOD1^{G37R}/YFP mice at
229 P360 were analyzed (Figure 3 and Table 2). Consistent with the *in vivo* results, α-motor neuron
230 degeneration and NMJ denervation were already severe at P360 in both male and female
231 SOD1^{G37R} mice (respectively, Figure 3A, C and E; *two-way ANOVA;* effect of genotype:
232 p=0.0002; Figure 3B, D and G; *GLM;* effect of genotype: p<0.001). Importantly, survival of γ-
233 motor neurons was unchanged in SOD1^{G37R}/YFP mice compared to WT/YFP mice, despite
234 females having slightly less γ-motor neurons in general (Figure 3F and Table 2; *two-way*
235 *ANOVA;* effect of genotype: p=0.673; effect of sex: p=0.0420).

236 Consistent with the grip strength results, we found that α-motor neuron degeneration was
237 increased in female SOD1^{G37R}/YFP mice compared to male SOD1^{G37R}/YFP mice (Figure 3E;
238 SOD1 males, 48% reduction, vs SOD1 females, 75% reduction; *ANOVA post-test;* p=0.0304),
239 even though the global interaction term was not significant (Table 2, *two-way ANOVA;*
240 interaction: p=0.9410). Similarly, loss of NMJ innervation in SOD1^{G37R}/YFP mice tended to be
241 greater in females than in males (Table 2, *GLM,* interaction; p=0.019), even though no specific
242 differences were observed between male and female SOD1^{G37R}/YFP mice (Figure 3G; SOD1
243 males vs SOD1 females; *GLM post-test*; p=0.121). Interestingly, NMJ innervation and α-motor
244 neuron counts were more variable in SOD1^{G37R}/YFP males than in SOD1^{G37R}/YFP females
245 (Figure 3E and G), further suggesting that some individual male mice may have been less
246 affected at that time point. In sum, these results confirm that α-motor neuron degeneration seems
247 to be more advanced in female than in male SOD1^{G37R}/YFP mice at P360.

248

249 **Discussion**

250 Our results show that female fast-fatigable MUs (surface of the *Tibialis anterior,* see
251 methods) are much more likely to form expansions in SOD1^{G37R}/YFP mice, resulting in a net
252 increase in MU size in females but not in males. This result is consistent with previous findings
253 on botulinum toxin-induced axonal sprouting (Moloney et al., 2017), where fast-fatigable motor
254 axons were more likely to sprout in female mice. Interestingly, this increased dynamism is
255 associated with an earlier onset of motor deficits and an exacerbated pathology in our female
256 mice, as shown by the loss of grip strength and the neuromuscular and spinal cord
257 histopathology. However, disease progression as measured by weight loss was equivalent in both
258 sexes, consistent with previous reports in loxSOD1^{G37R} mice (Lobsiger et al., 2013; Mesci et al.,
259 2015). These results suggest that excessive MU expansions may be maladaptive and detrimental
260 to motor neuron survival in the end.

261 Sex-specific differences have been identified in other SOD1 mouse models and in
262 patients carrying SOD1 mutations, but they did not consistently point toward a faster or more
263 severe disease in one sex (Hayworth and Gonzalez-Lima, 2009; Kim et al., 2012; Zwiegers et al.,
264 2014; Pfohl et al., 2015; Tang et al., 2019). For instance, male SOD1^{G93A} mice have an earlier
265 onset than female SOD1^{G93A} mice (Hayworth and Gonzalez-Lima, 2009; Kim et al., 2012; Pfohl
266 et al., 2015). Importantly, however, these differences depend on the presence of genetic
267 modifiers (Heiman-Patterson et al., 2005). Furthermore, female mice from another SOD1^{G37R}
268 line (line 29) have reduced survival and tend to have a delayed onset (Zwiegers et al., 2014),
269 which is reminiscent of our present finding in loxSOD1^{G37R} mice. These results contrast with a
270 recent study on Chinese familial ALS patients carrying SOD1 mutations which identified that
271 women tended to have a slower progression and longer survival after onset (Tang et al., 2019).

Of note though, a large proportion of male ALS patients in the Chinese population are smokers (44.7% vs 1.7% (Chen et al., 2015)) which has been previously associated with a substantial decrease (~ 1 year) in survival (de Jong et al., 2012). Hence, sex seems to affect SOD1-mediated ALS onset and progression via a complex and unclear interplay with several other factors, including the specific disease mutation, the genetic background and environmental risk factors.

A number of factors could explain our observations. One interesting possibility is that excessive MU expansions are detrimental to motor neuron survival. A previous study on dopaminergic neurons identified that large axonal arborization size is associated with increased energetic load and enhanced vulnerability in Parkinson's disease (Pacelli et al., 2015). Similarly, axonal length and complexity are predictive of NMJ vulnerability in ALS at the single motor neuron level (Tallon et al., 2016; Martineau et al., 2018). Hence, one could hypothesize that the excessive MU expansions in female SOD1^{G37R} mice could increase their energetic load during disease progression, exacerbating their stress. This possibility is consistent with the theoretical work of Le Masson et al. (2014) showing that local energetic imbalance in distal axonal branches in ALS could propagate and give rise to global energetic failures, contributing to global neuronal degeneration. According to their simulations, large motor axons had higher ATP consumption and were much more susceptible to this energetic imbalance than small motor axons (Le Masson et al., 2014). Interestingly, previous studies identified sex-specific differences in mitochondrial function in SOD1^{G93A} mice that have been suggested to underlie female resilience in this line. Notably, female SOD1^{G93A} mice have increased activation of the mitochondrial unfolded protein response (UPRmt) (Riar et al., 2017), reduced mitochondrial calcium accumulation (Kim et al., 2012) and improved preservation of complex I function (Cacabelos et al., 2016). However, whether these sex-specific differences in mitochondrial function are mutation- or genetic-

295 background-dependent remains to be determined. Nevertheless, together with the potential
296 expansion-induced increase in bioenergetic load, these results suggest that alterations in
297 mitochondrial function could contribute to the sex-linked phenotypic differences observed in
298 ALS animal models.

299 Alternatively, increased levels of neuronal loss in female SOD1^{G37R} mice, as observed at
300 P360, could in turn trigger more compensatory expansions from surviving MUs. This scenario
301 could also explain why females tended to have higher global levels of NMJ denervation despite
302 the similar amount of asynchronous NMJ losses between males and females. However, this
303 scenario is not entirely consistent with the notion that female fast-fatigable motor axons are
304 intrinsically more inclined to sprout (Moloney et al., 2017). Hence, additional studies aimed at
305 manipulating MUs expansions levels in males and females are required to determine whether
306 they represent an adaptive or a maladaptive response in female SOD1^{G37R} mice.

307 An important question is whether these findings on SOD1-mediated ALS are also
308 applicable to other genetic forms of ALS or to sporadic ALS. Sex-specific differences have been
309 observed in some non-SOD1 ALS mouse models and in the general ALS patient population, but
310 they are as discordant as those observed in SOD1-mediated ALS. For instance, disease
311 phenotype is more penetrant and rapidly progressing in females in one transgenic line of *C9orf72*
312 mice (Liu et al., 2016). However, studies on *C9orf72* patient cohorts report conflicting results,
313 with women having either a better (Rooney et al., 2017; Trojsi et al., 2019) or a worse
314 (Watanabe et al., 2015) survival time after onset. Likewise, the incidence of sporadic ALS, but
315 not familial ALS, is higher in men than in women, but bulbar-onset ALS is more common in
316 women and is associated with a poor prognosis (McCombe and Henderson, 2010; Kiernan et al.,
317 2011). Thus, as observed for SOD1-mediated ALS, sex seems to interact with several genetic

and clinical factors that shape disease progression, such as the site of onset and the disease mutation. Whether sex-specific differences in MU dynamics also occur in non-SOD1-mediated forms of ALS and contribute to this phenotypic heterogeneity would be an important aspect to evaluate.

Altogether, we identified here a novel factor to consider in our understanding of the conundrum that represents sex-specific differences in ALS progression. These findings highlight the need to clarify the prevalence of sex-specific difference by performing additional detailed analyses across animal models of the disease. Furthermore, future large-scale studies looking at the influence of sex on disease onset, progression and motor function in gene-specific ALS patient cohorts could shed light on abstruse animal data and further our understanding of ALS pathogenesis.

330 **References**

331

332 Armstrong GA, Drapeau P (2013a) Loss and gain of FUS function impair neuromuscular
333 synaptic transmission in a genetic model of ALS. Hum Mol Genet 22:4282-4292.
334 Armstrong GA, Drapeau P (2013b) Calcium channel agonists protect against neuromuscular
335 dysfunction in a genetic model of TDP-43 mutation in ALS. J Neurosci 33:1741-1752.
336 Cacabelos D, Ramirez-Nunez O, Granado-Serrano AB, Torres P, Ayala V, Moiseeva V,
337 Povedano M, Ferrer I, Pamplona R, Portero-Otin M, Boada J (2016) Early and gender-
338 specific differences in spinal cord mitochondrial function and oxidative stress markers in
339 a mouse model of ALS. Acta neuropathologica communications 4:3.
340 Chand KK, Lee KM, Lee JD, Qiu H, Willis EF, Lavidis NA, Hilliard MA, Noakes PG (2018)
341 Defects in synaptic transmission at the neuromuscular junction precede motor deficits in
342 a TDP-43(Q331K) transgenic mouse model of amyotrophic lateral sclerosis. FASEB J
343 32:2676-2689.
344 Chen L, Zhang B, Chen R, Tang L, Liu R, Yang Y, Yang Y, Liu X, Ye S, Zhan S, Fan D (2015)
345 Natural history and clinical features of sporadic amyotrophic lateral sclerosis in China. J
346 Neurol Neurosurg Psychiatry 86:1075-1081.
347 Clark JA, Southam KA, Blizzard CA, King AE, Dickson TC (2016) Axonal degeneration, distal
348 collateral branching and neuromuscular junction architecture alterations occur prior to
349 symptom onset in the SOD1(G93A) mouse model of amyotrophic lateral sclerosis.
350 Journal of chemical neuroanatomy 76:35-47.
351 Dantes M, McComas A (1991) The extent and time course of motoneuron involvement in
352 amyotrophic lateral sclerosis. Muscle Nerve 14:416-421.
353 de Jong SW, Huisman MH, Sutedja NA, van der Kooi AJ, de Visser M, Schelhaas HJ, Fischer K,
354 Veldink JH, van den Berg LH (2012) Smoking, alcohol consumption, and the risk of
355 amyotrophic lateral sclerosis: a population-based study. Am J Epidemiol 176:233-239.
356 Dengler R, Konstanzer A, Kuther G, Hesse S, Wolf W, Struppler A (1990) Amyotrophic lateral
357 sclerosis: macro-EMG and twitch forces of single motor units. Muscle Nerve 13:545-550.
358 Feng G, Mellor RH, Bernstein M, Keller-Peck C, Nguyen QT, Wallace M, Nerbonne JM,
359 Lichtman JW, Sanes JR (2000) Imaging neuronal subsets in transgenic mice expressing
360 multiple spectral variants of GFP. Neuron 28:41-51.
361 Fischer LR, Culver DG, Tennant P, Davis AA, Wang M, Castellano-Sanchez A, Khan J, Polak
362 MA, Glass JD (2004) Amyotrophic lateral sclerosis is a distal axonopathy: evidence in
363 mice and man. Exp Neurol 185:232-240.
364 Hayworth CR, Gonzalez-Lima F (2009) Pre-symptomatic detection of chronic motor deficits and
365 genotype prediction in congenic B6.SOD1(G93A) ALS mouse model. Neuroscience
366 164:975-985.
367 Hegedus J, Putman CT, Gordon T (2009) Progressive motor unit loss in the G93A mouse model
368 of amyotrophic lateral sclerosis is unaffected by gender. Muscle Nerve 39:318-327.
369 Heiman-Patterson TD, Deitch JS, Blankenhorn EP, Erwin KL, Perreault MJ, Alexander BK,
370 Byers N, Toman I, Alexander GM (2005) Background and gender effects on survival in
371 the TgN(SOD1-G93A)1Gur mouse model of ALS. J Neurol Sci 236:1-7.
372 Kim HJ, Magrane J, Starkov AA, Manfredi G (2012) The mitochondrial calcium regulator
373 cyclophilin D is an essential component of oestrogen-mediated neuroprotection in
374 amyotrophic lateral sclerosis. Brain 135:2865-2874.

375 Lalancette-Hebert M, Sharma A, Lyashchenko AK, Shneider NA (2016) Gamma motor neurons
376 survive and exacerbate alpha motor neuron degeneration in ALS. Proc Natl Acad Sci U S
377 A 113:E8316-E8325.
378 Le Masson G, Przedborski S, Abbott LF (2014) A computational model of motor neuron
379 degeneration. Neuron 83:975-988.
380 Liu Y, Pattamatta A, Zu T, Reid T, Bardhi O, Borchelt DR, Yachnis AT, Ranum LP (2016)
381 C9orf72 BAC Mouse Model with Motor Deficits and Neurodegenerative Features of
382 ALS/FTD. Neuron 90:521-534.
383 Lobsiger CS, Boillee S, McAlonis-Downes M, Khan AM, Feltri ML, Yamanaka K, Cleveland
384 DW (2009) Schwann cells expressing dismutase active mutant SOD1 unexpectedly slow
385 disease progression in ALS mice. Proc Natl Acad Sci U S A 106:4465-4470.
386 Lobsiger CS, Boillee S, Pozniak C, Khan AM, McAlonis-Downes M, Lewcock JW, Cleveland
387 DW (2013) C1q induction and global complement pathway activation do not contribute
388 to ALS toxicity in mutant SOD1 mice. Proc Natl Acad Sci U S A 110:E4385-4392.
389 Manjaly ZR, Scott KM, Abhinav K, Wijesekera L, Ganesalingam J, Goldstein LH, Janssen A,
390 Dougherty A, Willey E, Stanton BR, Turner MR, Ampong MA, Sakel M, Orrell RW,
391 Howard R, Shaw CE, Leigh PN, Al-Chalabi A (2010) The sex ratio in amyotrophic
392 lateral sclerosis: A population based study. Amyotroph Lateral Scler 11:439-442.
393 Martineau E, Di Polo A, Vande Velde C, Robitaille R (2018) Dynamic neuromuscular
394 remodeling precedes motor-unit loss in a mouse model of ALS. eLife 7.
395 McComas AJ, Sica RE, Campbell MJ, Upton AR (1971) Functional compensation in partially
396 denervated muscles. J Neurol Neurosurg Psychiatry 34:453-460.
397 McCombe PA, Henderson RD (2010) Effects of gender in amyotrophic lateral sclerosis. Gend
398 Med 7:557-570.
399 Mesci P, Zaidi S, Lobsiger CS, Millecamps S, Escartin C, Seilhean D, Sato H, Mallat M, Boillee
400 S (2015) System xC- is a mediator of microglial function and its deletion slows
401 symptoms in amyotrophic lateral sclerosis mice. Brain 138:53-68.
402 Moloney EB, Hobo B, De Winter F, Verhaagen J (2017) Expression of a Mutant SEMA3A
403 Protein with Diminished Signalling Capacity Does Not Alter ALS-Related Motor
404 Decline, or Confer Changes in NMJ Plasticity after BotoxA-Induced Paralysis of Male
405 Gastrocnemic Muscle. PLoS One 12:e0170314.
406 Pacelli C, Giguere N, Bourque MJ, Levesque M, Slack RS, Trudeau LE (2015) Elevated
407 Mitochondrial Bioenergetics and Axonal Arborization Size Are Key Contributors to the
408 Vulnerability of Dopamine Neurons. Curr Biol 25:2349-2360.
409 Pfohl SR, Halicek MT, Mitchell CS (2015) Characterization of the Contribution of Genetic
410 Background and Gender to Disease Progression in the SOD1 G93A Mouse Model of
411 Amyotrophic Lateral Sclerosis: A Meta-Analysis. J Neuromuscul Dis 2:137-150.
412 Pun S, Santos AF, Saxena S, Xu L, Caroni P (2006) Selective vulnerability and pruning of phasic
413 motoneuron axons in motoneuron disease alleviated by CNTF. Nat Neurosci 9:408-419.
414 Riar AK, Burstein SR, Palomo GM, Arreguin A, Manfredi G, Germain D (2017) Sex specific
415 activation of the ERalpha axis of the mitochondrial UPR (UPRmt) in the G93A-SOD1
416 mouse model of familial ALS. Hum Mol Genet 26:1318-1327.
417 Rivner MH, Liu S, Quarles B, Fleenor B, Shen C, Pan J, Mei L (2017) Agrin and low-density
418 lipoprotein-related receptor protein 4 antibodies in amyotrophic lateral sclerosis patients.
419 Muscle Nerve 55:430-432.

420 Rooney J, Fogh I, Westeneng HJ, Vajda A, McLaughlin R, Heverin M, Jones A, van Eijk R,
421 Calvo A, Mazzini L, Shaw C, Morrison K, Shaw PJ, Robberecht W, Van Damme P, Al-
422 Chalabi A, van den Berg L, Chio A, Veldink J, Hardiman O (2017) C9orf72 expansion
423 differentially affects males with spinal onset amyotrophic lateral sclerosis. J Neurol
424 Neurosurg Psychiatry 88:281.
425 Schmied A, Pouget J, Vedel JP (1999) Electromechanical coupling and synchronous firing of
426 single wrist extensor motor units in sporadic amyotrophic lateral sclerosis. Clinical
427 neurophysiology : official journal of the International Federation of Clinical
428 Neurophysiology 110:960-974.
429 Shneider NA, Brown MN, Smith CA, Pickel J, Alvarez FJ (2009) Gamma motor neurons express
430 distinct genetic markers at birth and require muscle spindle-derived GDNF for postnatal
431 survival. Neural Dev 4:42.
432 Tallon C, Russell KA, Sakhalkar S, Andrapallayal N, Farah MH (2016) Length-dependent axo-
433 terminal degeneration at the neuromuscular synapses of type II muscle in SOD1 mice.
434 Neuroscience 312:179-189.
435 Tang L, Ma Y, Liu XL, Chen L, Fan DS (2019) Better survival in female SOD1-mutant patients
436 with ALS: a study of SOD1-related natural history. Transl Neurodegener 8:2.
437 Tremblay E, Martineau E, Robitaille R (2017) Opposite Synaptic Alterations at the
438 Neuromuscular Junction in an ALS Mouse Model: When Motor Units Matter. J Neurosci
439 37:8901-8918.
440 Trojsi F et al. (2019) Comparative Analysis of C9orf72 and Sporadic Disease in a Large
441 Multicenter ALS Population: The Effect of Male Sex on Survival of C9orf72 Positive
442 Patients. Front Neurosci 13:485.
443 Watanabe H et al. (2015) Factors affecting longitudinal functional decline and survival in
444 amyotrophic lateral sclerosis patients. Amyotroph Lateral Scler Frontotemporal Degener
445 16:230-236.
446 Zwiegers P, Lee G, Shaw CA (2014) Reduction in hSOD1 copy number significantly impacts
447 ALS phenotype presentation in G37R (line 29) mice: implications for the assessment of
448 putative therapeutic agents. Journal of negative results in biomedicine 13:14.
449

450

Figure legends

Figure 1: Sex-specific differences in MU dynamics in female SOD1^{G37R}/YFP mice. A, Examples of MU arbors from a male and a female SOD1/YFP mice during three sessions (Male: session 2, 3 and 5; Female: session 2, 4 and 5), with higher magnification on-focus insets of NMJs of interest (digital zoom, dashed box in low magnification). Green: YFP-labeled axon; Red: nAChR. Note how the imaged motor axon retracted from two NMJs (arrowheads)between sessions 3 and 5 in the male example. Furthermore, note the formation of a new axonal branch between sessions 2 and 4 in the female example (arrow), innervating an NMJ that previously did not belong to this MU (MU expansion). **B**, MU dynamic diagram of the MUs shown in (**A**), showing that MU are much more likely to expand in female SOD1^{G37R}/YFP mice. Black lines represent the axonal arborization and each box represents a single NMJ. Note how asynchronous NMJ losses occurred in both these MUs, but how partial losses seem more frequent in the male MU. **C**, **D**, Histograms showing the average proportion of NMJs from the initial pool which are innervated (green), re-innervated (purple) or lost (red) by the MU and the proportion which are gained (blue) for female (**C**) and male (**D**) SOD1^{G37R}/YFP mice. Numbers in the histogram bars represent the number of remaining MU arbors (those which did not globally degenerate) over the total number of MUs observed. Again, note how MU expansions are more frequent in female than in male mice. Scale bar, low magnification: 100 µm; high magnification: 25 µm.

Figure 2: Motor function declines slightly faster in female SOD1^{G37R}/YFP mice. A and **B**, body weight (**A**) and all-limb grip strength (**B**) curves of male and female (light and dark colors respectively) WT/YFP and SOD1^{G37R}/YFP mice (blue and red respectively) during the symptomatic stages (WT female: N=14; WT male: N=6; SOD1 female: N=8; SOD1 male: N=12). Data are presented as mean ± SEM. Main effects and interactions are reported in Table 1 and in the text. Asterisks and crosses represent biologically relevant statistically significant differences in the post-test (Tukey's multiple comparisons). Asterisks represent differences compared to the other genotype, while crosses represent differences compared to the other sex. * / †: $p<0.05$; **/††: $p<0.01$; ***/†††: $p<0.001$; ****/††††: $p<0.0001$.

Figure 3: α-motor neuron loss and NMJ denervation are slightly more pronounced in female SOD1^{G37R}/YFP mice at P360. A, Representative image of lumbar spinal cord sections from a female WT/YFP mice at P360 (Red: ChAT; Blue: NeuN; Green: YFP). **B**, Representative image of NMJs in the *Tibialis anterior* muscle of a female WT/YFP mice at P360 (Red: α-BTX; Green: NF-M and SV2). **C,** Representative examples of lumbar spinal cord sections from female (top) and male (bottom) SOD1^{G37R}/YFP mice at P360. **D**, Representative images of NMJs in the *Tibialis anterior* muscle of female (top) and male (bottom) SOD1^{G37R}/YFP mice at P360. **E** and **F**, Quantification of the number of α-motor neurons (**E,** ChAT+ NeuN+ cells) and γ-motor neurons (**F**, ChAT+ NeuN- cells) per ventral horn at P360 (WT female: N=4; WT male: N=2; SOD1 female: N=4; SOD1 male: N=5). **G**, Quantification of the percentage of fully innervated NMJs in the *Tibialis anterior* at P360 (WT female: N=4, n=1078; WT male: N=2, n=446; SOD1

female: N=4, n=977; SOD1 male: N=5, n=820). Data are presented as mean ± SEM. Main effects and interactions are reported in Table 2 and in the text. Asterisks represent biologically relevant statistically significant differences in the post-test (E and F: Tukey's multiple comparisons; G: Holm-Sidak's correction). * : $p<0.05$; ** : $p<0.01$; *** : $p<0.001$. Scale bar: 100 µm.

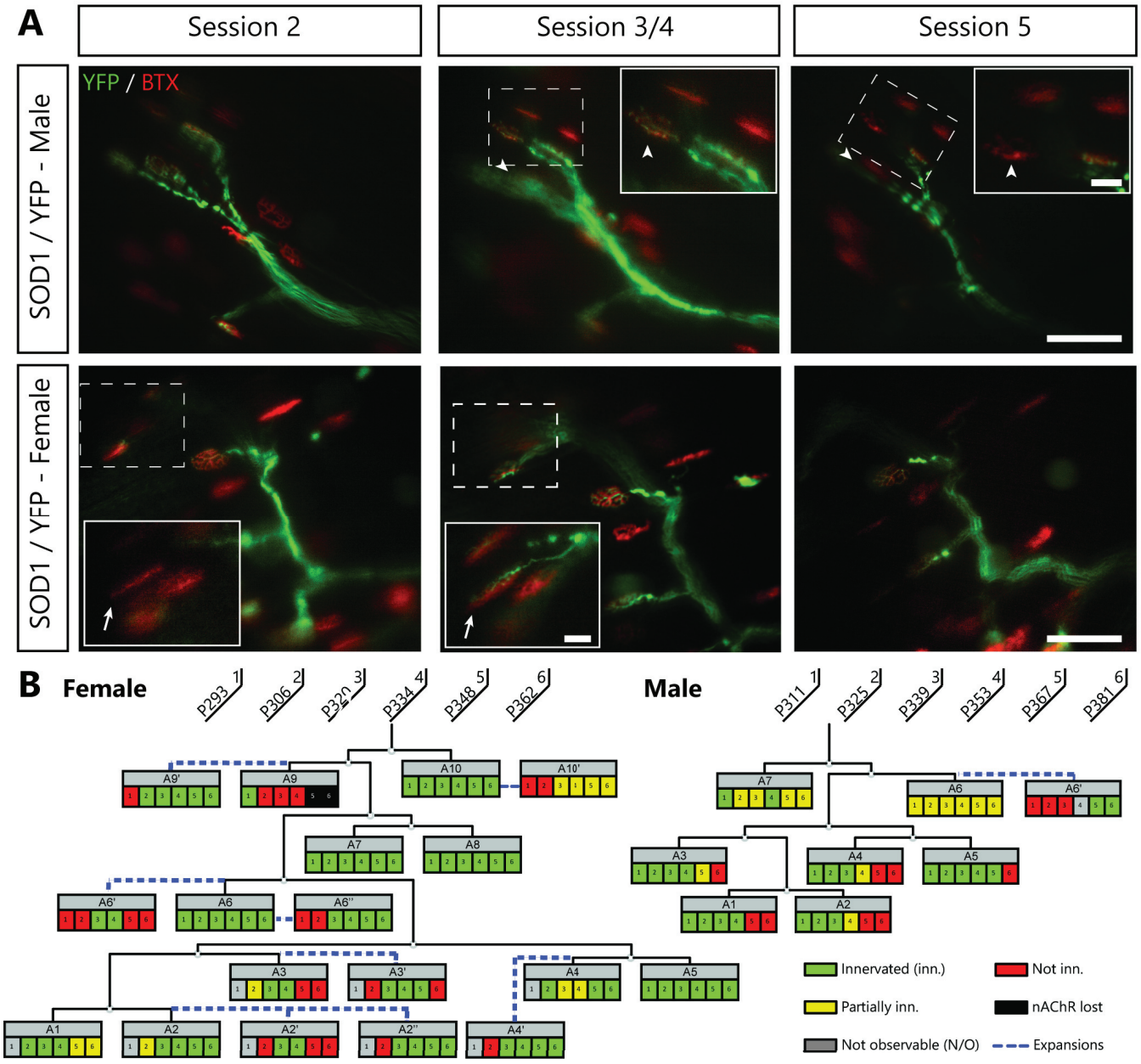

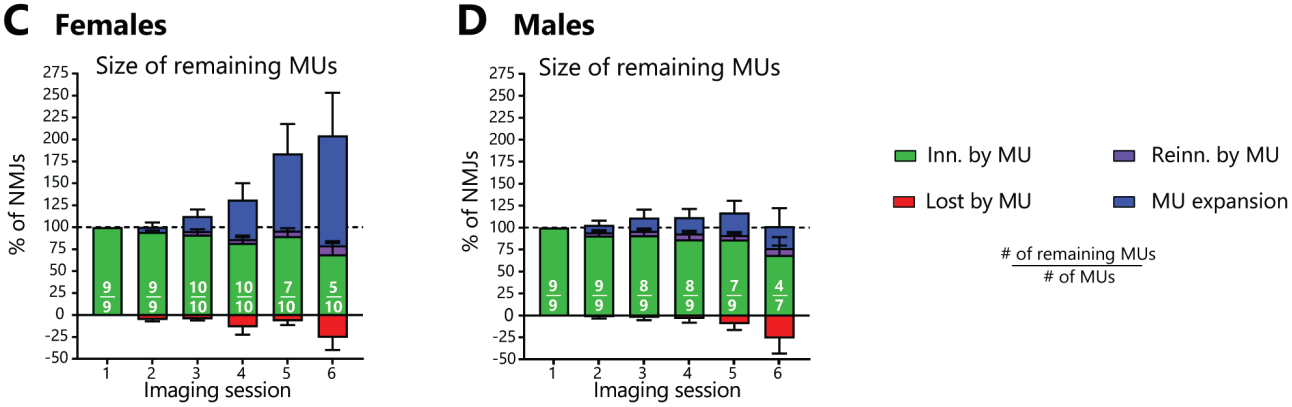

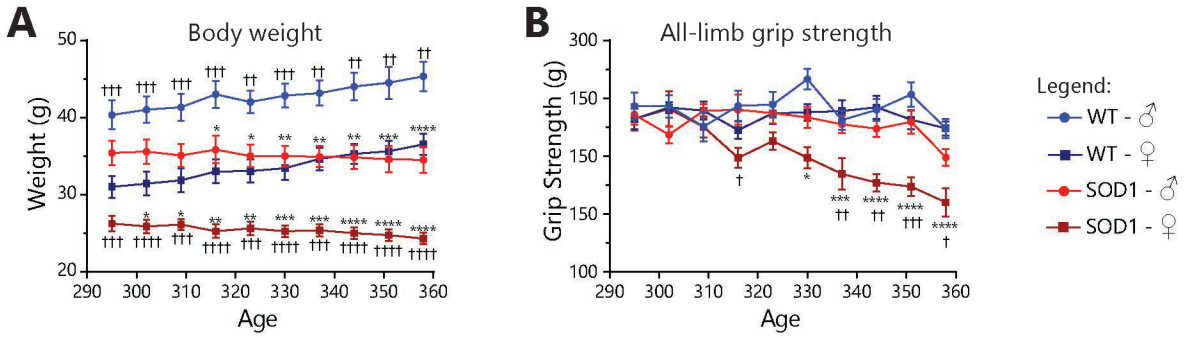

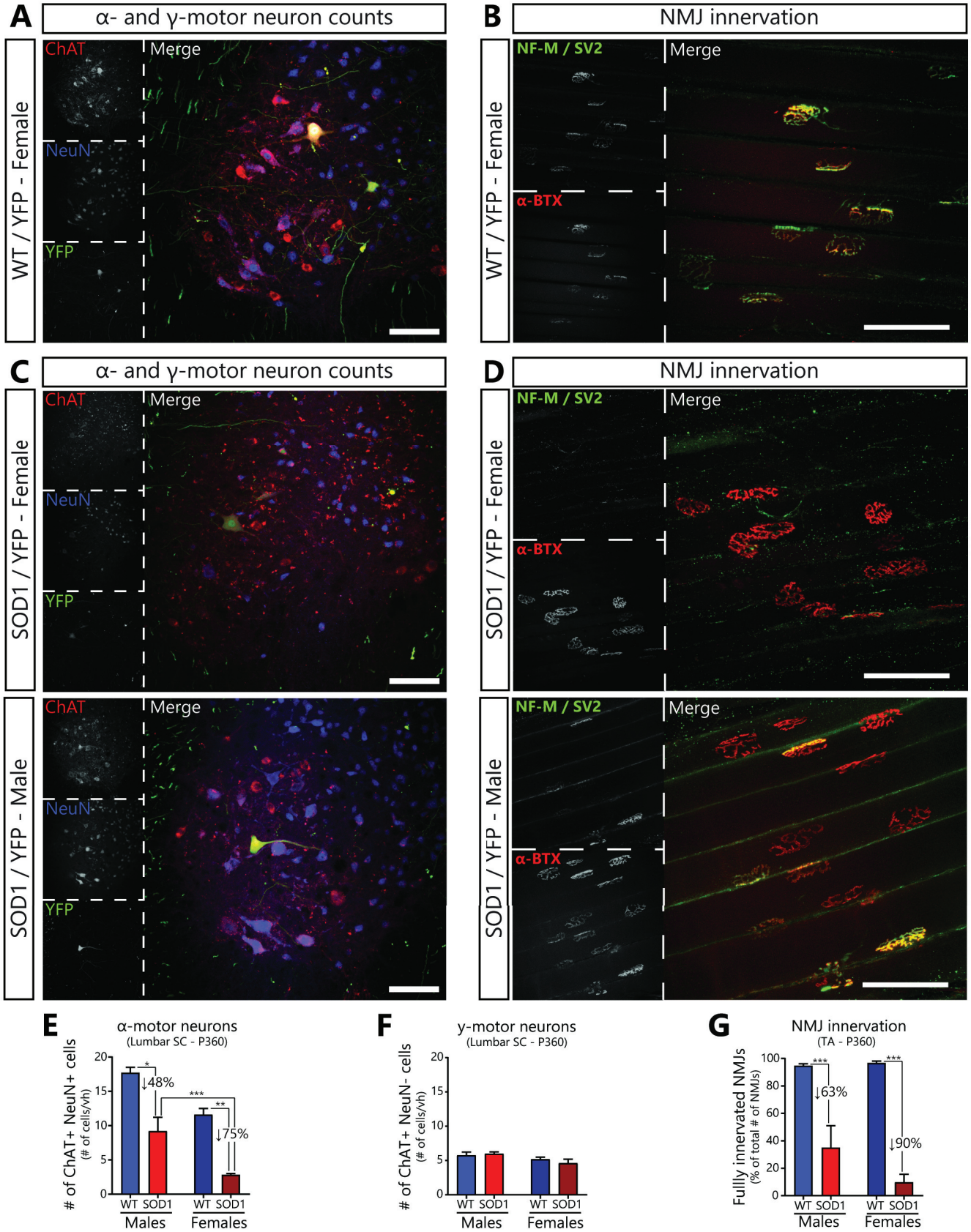

Table 1: Effect of time, sex and genotype on disease progression in SOD1^{G37R} mice.

Analysis	Statistical Test	Main effect	*p*-value
Body weight (Figure. 2A)	Repeated-measures three-way ANOVA	Time	**<0.001*** **
		Genotype	**<0.001*** **
		Sex	**<0.001*** **
		Time * Genotype	**<0.001*** **
		Time * Sex	0.854
		Sex * Genotype	0.868
		Time * Sex * Genotype	0.397
Grip strength (Figure. 2B)	Repeated-measures three-way ANOVA	Time	**<0.001*** **
		Genotype	**<0.001*** **
		Sex	**<0.001*** **
		Time * Genotype	**<0.001*** **
		Time * Sex	**0.007** **
		Sex * Genotype	**0.023* **
		Time * Sex * Genotype	**0.011* **

Table 2: Effect of sex and genotype on neuronal survival and NMJ innervation in SOD1^{G37R} mice.

Analysis	Statistical Test	Main effect	*p*-value
α-motor neurons counts (Figure. 3E)	Two-way ANOVA	Genotype	**<0.001*** **
		Sex	**0.002** **
		Sex * Genotype	0.941
γ-motor neurons counts (Figure. 3F)	Two-way ANOVA	Genotype	0.673
		Sex	**0.042* **
		Sex * Genotype	0.365
NMJ innervation (Figure. 3G)	GLM - logistic distribution	Genotype	**<0.001*** **
		Sex	0.431
		Sex * Genotype	**0.019* **